IEEE Access
Multidisciplinary | Rapid Review | Open Access Journal

Date of publication xxxx 00, 0000, date of current version xxxx 00, 0000.

Digital Object Identifier 00.0000/ACCESS.2019.DOI

PAPR-aware Massive MIMO-OFDM Downlink

RAFIK ZAYANI[1,2], (Member, IEEE) HMAIED SHAIEK[2], (Member, IEEE), DANIEL ROVIRAS[2], (Senior Member, IEEE)

[1]University of Carthage, Sup'Com, Innov'COM, Ariana 2083, Tunisia
[2]CNAM, CEDRIC/LAETITIA, Paris 75003, France

Corresponding author: Rafik Zayani (e-mail: rafik.zayani@supcom.tn).

This work has been performed in the framework of the ADAM5 project, receiving funds from the European Union under H2020-EU.1.3.2 with funding scheme MSCA-IF-EF-ST (Project ID: 796401)

ABSTRACT We investigate the peak-to-average power ratio (PAPR) reduction problem in orthogonal frequency-division multiplexing (OFDM) based massive multi-user (MU) multiple-input multiple-output (MIMO) downlink systems. In this paper, we develop a downlink transmission scheme that performs jointly MU precoding and PAPR reduction (PP) by exploiting the excess degrees of freedom (DoF) offered by equipping the BS by a large number of antennas. Specifically, the joint MU precoding and PAPR reduction scheme is formulated as a simple convex optimization problem solved via steepest gradient descent (GD) approach. Then, we develop a novel algorithm, referred to as MU-PP-GDm, to reduce the PAPR of the transmitted signals by exploiting the high-dimensional null-space of the MIMO channel matrix while maintaining excellent transmission quality. Simulation results show that the proposed MU-PP-GDm has a low computational complexity and can achieve substantial PAPR performance with fast convergence rate.

INDEX TERMS 5G+, massive multiple-input multiple-output (MIMO), orthogonal frequency-division multiplexing (OFDM), peak-to-average power ratio (PAPR), multi-user (MU) precoding, convex optimization, gradient descent (GD).

I. INTRODUCTION

Massive multiple-input multiple-output (MIMO), also known as large-scale multi-user (MU) MIMO, has been recognized as a promising technology for future generations of wireless communications. It has been initially introduced in [1] and popularly studied in [2] where a large number of antennas are employed at the base station (BS) simultaneously serving a much smaller number of single-antenna users using MU precoding. Wireless massive MIMO systems enable the use of low-cost and low-power single-antenna user devices while expensive equipment is only needed on the BS. In this way, potential improvements are provided in the spectral- and energy- efficiency [3]. Furthermore, simple linear signal processing approaches, such as matched filter (MF), minimum mean-squared error (MMSE) and zero-forcing (ZF), can be used as precoding techniques for massive MIMO downlink that have the potential to reduce the operational power consumption at the transmitter and enable the suppression of MU interference (MUI) [4].

In practice, broadband wireless communications, however, encounter large delay spread, and, therefore, suffer from frequency-selective fading. Orthogonal frequency-division multiplexing (OFDM), a scheme of encoding digital symbols on multiple orthogonal sub-carriers, is an efficient and well-established way to deal with frequency-selective channels. Therefore, massive MIMO-OFDM is a very promising combination to meet the ever growing demands for higher link readability and spectrum efficiency of next-generation wireless communication systems (5G and Beyond).

However, massive MIMO precoders exhibit transmit signals with high peak-to-average power ratio (PAPR), regardless of whether single-carrier or OFDM transmission and of whether a low or a high modulation order is used [4]. Consequently, the nonlinearity of the radio frequency (RF) high-power amplifier (HPA), which is necessary in a transmission chain, yields in-band distortion and out-of-band radiation (OBR) which cause signal distortion, phase rotation and adjacent channel interference, respectively. To avoid such heavy distortions, the transmit signals require that the power amplifiers are backed-off and operated in their linear region (i.e., where their transfer characteristics are sufficiently linear). Nevertheless, operating at lower power levels reduces

the power efficiency, which would result in huge operational expenditure for large-scale BS having hundreds of antennas. This is not a practical solution for 5G networks since the target energy efficiency improvement is 100x w.r.t. 4G long-term evolution (LTE) [5]. Therefore, it is primordial to reduce the PAPR of OFDM-based massive MIMO systems to motivate corresponding energy- and cost- efficient massive MIMO BS deployments. Thus, low-PAPR MU precoders would be of paramount importance since massive MIMO systems have the potential to reduce the PAPR of transmit signals by exploiting the excess spatial degrees-of-freedom (DoFs) [2].

Over the recent past years, many efforts have been devoted to introduce MU-MIMO precoding based PAPR reduction schemes because joint signal processing at the receiver side is impossible as users are spatially distributed. Low-PAPR Tomlinson-Harashima precoding schemes suitable for MU-MISO and MU-MIMO downlink were initially described in [6] and [7], respectively. These schemes, however, require specific signal processing at the receiver side (i.e. in the mobile terminal) making them less attractive. In [8], authors have proposed a peak-signal clipping scheme for PAPR reduction in OFDM-based massive MIMO where some of the antennas at the BS are reserved to compensate for peak-clipping signals. Another method has been introduced in [9] that aims at reserving some tones to reduce the PAPR in large-scale MU-MIMO-OFDM systems. Despite of their low computational complexity, these methods are lose efficiency since they sacrifice spectral efficiency by reserving some antennas or some tones, which are not realistic solutions for future wireless networks. In [10], Studer et al. have introduced a downlink transmission scheme for massive MU-MIMO-OFDM wireless systems. The proposed fast iterative truncation (FITRA) [10] algorithm aims to perform jointly MU precoding, OFDM modulation and PAPR reduction (PMP). This method provides good PAPR performance by sacrificing the transmission quality (MUI) and affecting the spectral purity (i.e. OBR). Moreover, the complexity of this algorithm is high. Authors in [11] have developed an efficient approximate passing (AMP)-based Bayesian method (EM-TGM-GAMP) [11] for joint PAPR reduction and MUI cancellation for massive MIMO-OFDM, which has been demonstrated to show better performance compared to FITRA, in terms of convergence speed and PAPR reduction performance. More recently, an efficient perturbation-assisted based alterative direction method of multipliers (ADMM) technique [12] has been proposed to address PAPR reduction for large-scale MU-MIMO-OFDM. The proposed PROXIINF-ADMM [12] algorithm has the advantage to do not cause any additional in-band distortion (MUI) and out-of-band radiations while its performance is very close to those provided by FITRA. However, PROXIINF-ADMM still has a quite high computational complexity, even if, it has a faster convergence speed compared to FITRA and EM-TGM-GAMP.

Motivated by these considerations, it is encouraged to concentrate on the development of an efficient MU precoding scheme based PAPR reduction that aims at performing jointly the MU precoding and the PAPR reduction without sacrificing neither the spectral efficiency nor the transmission quality nor the spectral purity. It should exploit the extra null-space of the associated massive MIMO channel [13]. A big emphasis should be put on reducing the computational complexity.

In this paper, we develop a downlink transmission scheme to address the PAPR reduction problem for OFDM-based massive MIMO wireless systems, which leaves the processing required at each mobile terminal untouched while affecting only the signal processing at the BS. Our proposed method performs jointly MU precoding and PAPR reduction that are formulated as a convex optimization problem and solved online with instantaneous processed data via gradient descent (GD) approach. On one hand, it aims at optimizing frequency-domain precoded signals that perfectly remove all MUI, guaranteeing ideal transmission quality, and spectral purity. On another hand, it introduces carefully, to precoded signals, frequency-domain peak-cancelling signals that are conceived to reduce the PAPRs of the transmitted symbols. The additive peak-power signals are restricted to only the null-space of their associated MIMO channel matrices. This restriction guarantees that the additive peak-power signals do not cause any additional MUI. We formulate the design of these additive peak-power signals as constrained convex optimization problems that is solved via GD approach. The optimization of the two sets of signals is done jointly since they perform in different orthogonal spaces. In this regard, we develop a novel optimization algorithm, referred to as MU precoding based PAPR reduction via gradient descent approach (MU-PP-GDm), which is able to find efficient solution to MU-PP for large-scale MU-MIMO-OFDM.

Compared with existing methods, e.g. [7]- [12], our proposed method presents the following improvements:

- The substantial improvement is related to the fact that our method has a lower computational complexity over all existing methods when considering a given PAPR performance target. Indeed, only matrix-vector multiplications are performed when using the GD-based solver, avoiding the computation of large-scale pseudo-inverse matrix. For example, the PROXIINF-ADMM [12] initializes the frequency-domain precoded signals using the zero-forcing (ZF) precoding scheme that aims at eliminating the MUI completely, but with high computational complexity. A low computational complexity precoder is an interesting merit for practical systems.
- Our proposed method guarantees perfect MUI cancellation and do not cause any additional out-of-band radiations, whereas, other proposed method (e.g., [10] and [11]) can not guarantee complete MUI cancellation and any OBR. Such precoder is of paramount importance for future wireless networks.
- Most PAPR reduction schemes for massive MIMO-OFDM [10] [12] use some appropriate regularization or penalty parameters, which are manually adjusted. In

contrast, in our proposed algorithm all parameters are adjusted automatically leading to a faster convergence to the optimal PAPR while maintaining excellent transmission quality.

The rest part of this paper is structured as follows. Section II provides the system model, the MU precoding scheme and the PAPR reduction problem. In section III, the proposed approach-assisted MU precoding and PAPR reduction are formulated as convex optimization problems. The developed MU-PP-GDm algorithm is discussed in section IV. Simulation results are provided in section V. Finally, the conclusion is given in section IV.

Notations : Lowercase boldface letters (e.g. $\mathbf{x}$) stand for column vectors, bold lowercase letters with a superscript $(.)^t$ (e.g. $\mathbf{x}^t$) denotes row vectors, and bold uppercase letters (e.g. $\mathbf{X}$) denotes matrices. We denote its transpose, conjugate transpose, pseudo-inverse and largest singular value by $\mathbf{X}^T$, $\mathbf{X}^H$, $\mathbf{X}^\dagger$ and $\sigma_{max}(\mathbf{X})$, respectively. For a $M \times N$-dimensional matrix $\mathbf{X} = \{x_{mn}\}$, we use $\mathbf{x}_m$ to designate the m-th column, and $\mathbf{x}_n^t$ to designate the n-th row. The $N \times N$ identity matrix and the $M \times N$ all-zeros matrix are denoted by $\mathbf{I}_N$ and $\mathbf{0}_{M\times N}$, respectively. We use $\|\mathbf{x}\|_2$ and $\|\mathbf{x}\|_\infty$ to denote l_2-norm and l_∞-norm of vector $\mathbf{x}$, respectively. The cardinality and complement of set χ is $|\chi|$ and χ^c, respectively. $\mathbb{E}[.]$ stands for the expectation operator.

II. PRELIMINARIES

A. SYSTEM MODEL

We consider a typical OFDM-based massive MIMO downlink scenario as illustrated in Fig. 1. We assume that the BS is equipped with M_t transmit antennas and simultaneously serves M_r single-antenna terminals (users) over a frequency-selective channel, where M_t is significantly larger than M_r. The signal vector $\mathbf{s}_n \in \mathbb{C}^{M_r\times 1}$ contains the symbols associated with the n-th tone for M_r users, where $n = 1, ..., N$ indexes the OFDM subcarriers, N denotes the total number of OFDM tones. $\mathbf{s}_n$ is chosen from a complex-valued constellations $\mathcal{A}$. In practice, OFDM systems typically specify certain unused subcarriers, which are used for guard-band (e.g., at both ends of the spectrum). Hence, the set of subcarriers available are divided into two sets χ and χ^c, where the subcarriers in set χ are used for data transmission and the subcarriers in its complementary set χ^c are used for guard-band. Moreover, we set $\mathbf{s}_n = \mathbf{0}_{M_r\times 1}$ for $n \in \chi^c$ such that no signal is transmitted on the guard-band.

B. MULTI-USER PRECODING SCHEME

To remove MUI at the receivers, precoding needs to be performed at the BS since cooperative detection among users is often impossible. The signal vectors $\mathbf{s_n}, \forall n$, can be linearly precoded as

$$\mathbf{c}_n = \frac{1}{\sqrt{\varsigma_W}}\mathbf{W}_n\mathbf{s}_n \tag{1}$$

where $\mathbf{c_n} \in \mathbb{C}^{M_t\times 1}$ represents the precoded vector that contains symbols to be transmitted over the n-th subcarrier through the M_t antennas, $\mathbf{W_n} \in \mathbb{C}^{M_t\times M_r}$ denotes the precoding matrix for n-th OFDM subcarrier and ς_W is a normalization factor designed to obtain an average or instantaneous transmit power equal to σ_s^2 .

Zero-forcing (ZF) precoding scheme is considered in this paper, which aims at cancelling the MUI completely. Note that since $M_r \ll M_t$, there are many precoding matrices that can achieve perfect MUI elimination, where the most widely used form is

$$\mathbf{W_n} = \mathbf{H}_n^H\left(\mathbf{H}_n\mathbf{H}_n^H\right)^{-1} \tag{2}$$

where $\mathbf{H}_n \in \mathbb{C}^{M_r\times M_t}$ is the MIMO channel matrix associated with the n-th OFDM subcarrier. Here, we assume that the channel matrices $\{\mathbf{H}_n\}$ are perfectly known at the BS, which can be determined by exploiting the channel reciprocity [14] [15] of time division multiplexing (TDD) systems.

It can be easily verified that the ZF has a high computational complexity [16] [17] since it needs to compute large-scale pseudo-inverse matrix.

After precoding, the M_t-dimensional vectors $\mathbf{c}_n$, $\forall n$ are reordered to M_t transmit antennas for OFDM modulation, according to the following one-to-one mapping

$$\left[\mathbf{x}_1^t ... \mathbf{x}_{M_t}^t\right] = \left[\mathbf{c}_1 ... \mathbf{c}_N\right]^T \tag{3}$$

Here, the N-dimensional vector $\mathbf{x}_{m_t}$ denotes the frequency-domain signal to be transmitted from m_t-th antenna. The time-domain signal $\{\mathbf{a}_{m_t}^t\}$ is obtained by applying an inverse fast Fourier transform (IFFT) of $\{\mathbf{x}_{m_t}^t\}$. Prior the transmission over wireless channel, a cyclic-prefix (CP) is added to the time-domain samples of each antenna in order to avoid inter-symbol interference (ISI).

To simplify the presentation and without loss of generality, we specify the input-output relation of wireless channel in frequency-domain only. Then, the signal received by M_r users can be expressed as

$$\mathbf{y}_n = \mathbf{H}_n\mathbf{c}_n + \mathbf{b}_n, \qquad n \in \chi \tag{4}$$

where $\mathbf{b}_n \in \mathbb{C}^{M_r\times 1}$ represents the receiver noise whose entries are i.i.d circularly-symmetric complex Gaussian distribution with zero-mean and variance $N_0/2$.

Since $\mathbf{H}_n\mathbf{H}_n^\dagger = \mathbf{I}_{M_r}$, transmitting $\mathbf{c}_n = \mathbf{H}_n^\dagger\mathbf{s}_n$ perfectly removes all MUI. Then, (4) can be transformed into M_r independent single-stream formulation and it can be rewritten as

$$\mathbf{y}_n = \mathbf{s}_n + \mathbf{b}_n, \qquad n \in \chi \tag{5}$$

Note that the precoded vectors $\mathbf{c}_n$ needs to satisfy

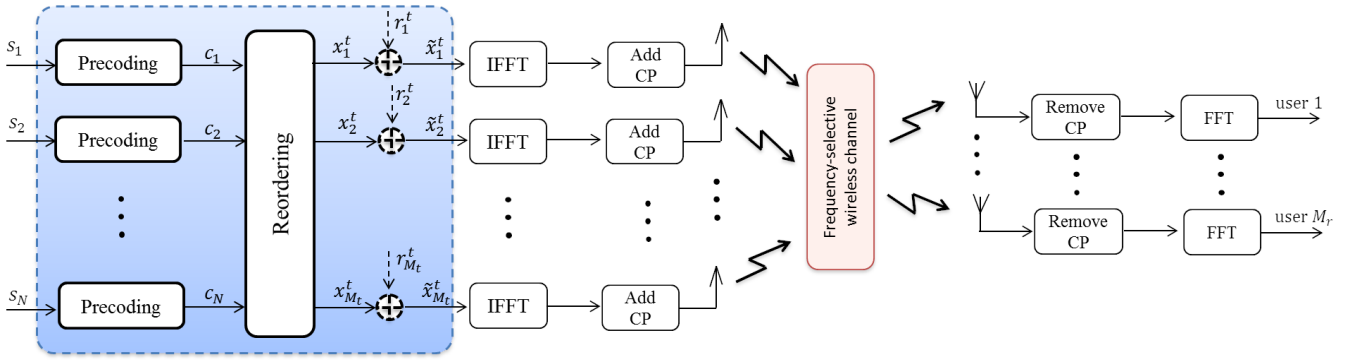

FIGURE 1. System model of the massive MIMO-OFDM downlink: M_t transmit antennas at the BS, M_r independent single-antenna terminals, N OFDM tones. The proposed MU-PP-GD, highlighted by the dashed box in the BS, combines MU precoding and PAPR reduction.

$$\begin{aligned} \mathbf{s}_n &= \mathbf{H}_n \mathbf{c}_n, \qquad n \in \chi \\ \mathbf{c}_n &= \mathbf{0}_{M_t \times 1}, \qquad n \in \chi^c \end{aligned} \tag{6}$$

Note that this is equivalent to transmitting $\{\mathbf{x}_n, \forall n\}$ that satisfy

$$\mathbf{s}_n = \mathbf{H}_n \mathbf{x}_n, \qquad n \in \chi \tag{7}$$

where $\mathbf{x}_n \in \mathbb{C}^{M_t \times 1}$ denotes the frequency-domain precoded signal associated with M_t transmit antennas at the n-th subcarrier.

In order to ensure desirable spectral properties of the transmitted OFDM signals, the inactive OFDM subcarrier (indexed by χ^c) must satisfy the following shaping constraints

$$\mathbf{x}_n = \mathbf{0}_{M_t \times 1}, \qquad n \in \chi^c \tag{8}$$

Consequently, the total MUI energy can be evaluated by $\|\mathbf{H}_n \mathbf{x}_n - \mathbf{s}_n\|_2^2, \forall n$. Note that ZF precoding is equivalent to transmitting the solution $\dot{\mathbf{x}}_n$ to the following convex optimization problem

$$\begin{aligned} \underset{\dot{\mathbf{x}}_n}{minimize} \quad & F(\mathbf{x}_n) = \|\mathbf{H}_n \mathbf{x}_n - \mathbf{s}_n\|_2^2, \qquad n \in \chi \\ subject\ to \quad & \mathbf{x}_n = \mathbf{0}_{M_t \times 1}, \qquad n \in \chi^c \end{aligned} \tag{9}$$

This formulation inspired us to state the MU massive MIMO precoding scheme as a convex optimization problem that can be solved online with instantaneous scenario information (i.e., transmit data, CSI). This would have a lower computational complexity and, most importantly, it will enable to perform the PAPR reduction in a flexible way, as discussed in Section III.

C. PEAK TO AVERAGE POWER RATIO

Consider a typical OFDM system with N subcarriers. The oversampled OFDM symbol in discrete time-domain $\mathbf{a}_{m_t}^t = [a_{m_t 0}, a_{m_t 1}, ..., a_{m_t LN-1}]$ at m_t-th transmit antenna , where the oversampling factor is denoted as L, is generated by LN-point inverse fast Fourier transform (IFFT) operation as

$$a_{m_t}(k) = \frac{1}{\sqrt{LN}} \sum_{n=0}^{N-1} \tilde{x}_{m_t}(n) e^{\frac{j2\pi nk}{LN}}, \quad 0 \le k \le LN-1 \tag{10}$$

where $\tilde{\mathbf{x}}_{\mathbf{m_t}}$ is the algorithm solution, k stands for a discrete time index and $j = \sqrt{-1}$. The OFDM signal can also be written in matrix form as

$$\underbrace{\mathbf{a}_{m_t}^t}_{[LN \times 1]} = \underbrace{\mathbf{F}^{\mathbf{H}}}_{[LN \times N]} \underbrace{\tilde{\mathbf{x}}_{m_t}^t}_{[N \times 1]}, \tag{11}$$

where $\mathbf{F}^{\mathbf{H}}$ denotes the $LN \times N$ IFFT matrix. A normalization is applied to the frequency-domain signal to ensure fixed transmit power.

The PAPR of $\mathbf{a}_{m_t}^t$ is defined as the ratio of the highest signal peak power to its average power value. Hence, it is given by

$$PAPR(\mathbf{a}_{m_t}^t) = \frac{\underset{0 \le k \le LN-1}{max} \left[|a_{m_t}(k)|^2\right]}{\mathbb{E}\left[|a_{m_t}(k)|^2\right]} = \frac{LN \|\mathbf{a}_{m_t}^t\|_\infty^2}{\|\mathbf{a}_{m_t}^t\|_2^2}, \tag{12}$$

Existing PAPR reduction methods, e.g. [6]- [11], for massive MU-MIMO-OFDM systems performs directly through performing the precoded signals $\{\mathbf{c}_n\}$. The key idea behind all these methods is that, due to the redundant DoFs rendered by the large number of antennas at the BS, there exist a great number of precoded signals that can achieve perfect MUI cancellation, from which we may find a set of precoded signals $\{\mathbf{c}_n\}$ whose time-domain counterpart signals $\{\mathbf{a}_{m_t}^t\}$ have a low PAPR. Recently, a solution was introduced in [12], which consists on a perturbation-assisted scheme that does not rely on the precoding design to reduce the PAPR. However, either they rely on the precoding design or not, these approaches may have limited applicability because, in practical systems, the precoding matrices can be either chosen from a pre-specified codebook or according a specified criterion that could be performed online. In this regard, in

the next section, we propose a MU precoding scheme based PAPR reduction that is transparent to the precoding design.

III. PROPOSED JOINT PRECODING AND PAPR REDUCTION ALGORITHM

A. DISCUSSION

The key idea of the proposed downlink transmission scheme is to exploit the high-dimensional null-space of the massive MIMO channel matrix offered by equipping the BS with a large number of antennas and to jointly perform MU precoding and PAPR reduction. Therefore, it aims to compute the precoded signals $\{\mathbf{x}_{m_t}^t\}$ that satisfy $\{\mathbf{H}_n\mathbf{c}_n = \mathbf{s}_n\}$ (where $\{\mathbf{c}_n\}$ are the reordered versions of $\{\mathbf{x}_{m_t}^t\}$) and evaluates the peak-canceling signals $\{\mathbf{r}_{m_t}^t\}$ that reduces the PAPR of the resulting time-domain signal $\{\mathbf{a}_{m_t}^t\}$ (see Fig. 1). It is worth to mention that the peak-canceling signals $\{\mathbf{r}_{m_t}^t\}$ are constrained to lie in the null-space of their associated MIMO channel matrices such that they do not disturb the signals received by M_r users through the N subcarriers (i.e. they are transparent to the receivers). Thus, adding the peak-canceling signals does not damage the transmission quality (i.e., MUI and capacity) since they vanish after propagating through the wireless channel. We next formulate the convex optimization problem, which jointly performs MU precoding and PAPR reduction, while enabling the use of conventional OFDM demodulation at the receivers.

We start by specifying the necessary constraints. To completely remove MUI and ensure spectral purity, the precoding constraints in (7) and (8) must hold, which leads to the convex optimization problem in (9). PAPR reduction is achieved by adding peak-canceling signals $\{\mathbf{r}_{m_t}^t\}$ to precoded signals $\{\mathbf{x}_{m_t}^t\}$. Specifically, the N-dimensional vector $\mathbf{r}_{m_t}^t$ is the peak-canceling signal added to the precoded signal of the m-th transmit antenna, while $\mathbf{r}_n \in \mathbb{C}^{M_t\times 1}$ is the peak-canceling signal added to the precoded signal associated to the n-th subcarrier, i.e. $\mathbf{x}_n$. In order to avoid any in-band distortions (i.e., MUI), the peak-canceling signals must satisfy the following conditions

$$\mathbf{H}_n\mathbf{r}_n = \mathbf{0}_{M_r\times 1}, \qquad n \in \chi \tag{13}$$

Note that $\mathbf{H}_n$ can be decomposed by using singular value decomposition (SVD) [18] as

$$\mathbf{H}_n = \mathbf{U}_n\mathbf{\Sigma}_n\mathbf{V}_n^H, \qquad \forall n \tag{14}$$

where $\mathbf{U}_n$ is an $M_r \times M_r$ complex unitary matrix, $\mathbf{\Sigma}_n$ is an $M_r \times M_t$ rectangular diagonal matrix with non-negative real numbers on the diagonal, and $\mathbf{V}_n^H = \left[\mathbf{v}_n^1, \mathbf{v}_n^2, ..., \mathbf{v}_n^{M_t}\right]$ is an $M_t \times M_t$ complex unitary matrix. The diagonal entries σ_i of $\mathbf{\Sigma}_n$ are known as the singular values of $\mathbf{H}_n$.

Note that MIMO transmission uses $M_t \times M_r$-dimensional $\mathbf{V}_n^d = \left[\mathbf{v}_n^1, \mathbf{v}_n^2, ..., \mathbf{v}_n^{M_r}\right]$ as the Beamforming (BF) matrix of the M_r data streams. On the other hand, the $M_t \times (M_t - M_r)$-dimensional $\mathbf{V}_n^0 = \left[\mathbf{v}_n^{M_r+1}, ..., \mathbf{v}_n^{M_t}\right]$ spans the null-space of the channel since it is not used for BF of the data streams. Therefore

$$\mathbf{H}_n\mathbf{V}_n^0 = \mathbf{0}, \qquad \forall n \tag{15}$$

In the following, we will represent $\mathbf{r}_n$ by using a $(M_t - M_r)$-dimensional vector $\mathbf{e}_n$ as

$$\mathbf{r}_n = \mathbf{V}_n^0\mathbf{e}_n \tag{16}$$

Moreover, to avoid spectral regrowth, i.e. out-of-band radiations, the following constraint must hold on the guard bands (indexed by χ^c)

$$\mathbf{r}_n = \mathbf{0}_{M_t\times 1}, \qquad n \in \chi^c \tag{17}$$

A conventional demodulation OFDM is sufficient and no additional processing is needed at the receivers by holding the above constraints. That is, the peak-canceling signals are transparent to the receivers.

Here, we wish to minimize the PAPR at each antenna. Then, we take an approach that minimizes the largest magnitude of the time domain-signals $\{\mathbf{a}_{m_t}^t\}$. This results is a sub-optimal solution that leads to a convex formulation while it can substantially reduce the PAPR [10]. In fact, directly optimizing (12), i.e. minimize jointly the PAPRs associated with all antennas, results in a non-convex problem which is not straightforward to solve and, to our best knowledge, there is no efficient solution for such a non-convex problem.

In the following, we discuss how to design the peak-canceling signals $\{\mathbf{r}_n\}$. The key idea is to iteratively fit the peak-canceling signals to their associated frequency-domain clipping-noise signals. These latter are obtained by clipping the time-domain signals $\{\mathbf{a}_{m_t}^t\}$. Given the clipping threshold λ, the clipped signal $\bar{\mathbf{a}}_n$ at the n-th subcarrier can be obtained by

$$\bar{a}_{m_t}(k) = \begin{cases} a_{m_t}(k), & if\ |a_{m_t}(k)| < \lambda \\ \lambda e^{j\phi(k)}, & if\ |a_{m_t}(k)| > \lambda \end{cases}, \tag{18}$$

where $a_{m_t}(k) = |a_{m_t}(k)|e^{j\phi(k)}$ and $\phi(k)$ is the phase of $a_{m_t}(k)$. In order to obtain the best PAPR, the optimal clipping threshold [19] λ is closely related with the mean power of the OFDM signal σ_a^2 and the ratio of the used subcarriers $\frac{N}{|\chi^c|}$ and is given by

$$\lambda = \sigma_a\sqrt{ln\left(\frac{N}{|\chi^c|}\right)} \tag{19}$$

Evidently, the original frequency-domain clipping noise associated to the m_t-th transmit antenna is $\mathbf{d}_{m_t}^t = FFT\left(\bar{\mathbf{a}}_{m_t} - \mathbf{a}_{m_t}\right)$. Then, the optimal peak-canceling signals

$$\mathbf{V}_n^0\mathbf{e}_n = \mathbf{d}_n, \qquad \forall n \in \chi \tag{20}$$

where $\mathbf{d}_n$ contains samples associated to the n-th subcarrier collected from the M_t vectors $\left(\mathbf{d}_1^t, \mathbf{d}_2^t, ..., \mathbf{d}_{M_t}^t\right)$.

Then, the effective transmission signal $\tilde{\mathbf{x}}_n$ at the n-th subcarrier in the frequency-domain is represented as

$$\tilde{\mathbf{x}}_n = \mathbf{x}_n + p_n \mathbf{V}_n^0 \mathbf{e}_n, \qquad n \in \chi \tag{21}$$

where p_n is a regularization factor. In fact, the peak-canceling signals during the first iteration is much smaller than that of the original clipping noises when the traditional clipping control (CC) method is employed in OFDM systems. Hence, this regularization factor aims at generating the optimal peak-canceling signals with fast convergence. The regularization factor is calculated using least-squares approximation (LSA) [20] and it is defined as

$$p_n = \frac{\sum_k |\mathbf{V}_n^0 \mathbf{e}_n||\mathbf{d}_n|}{\sum_k |\mathbf{V}_n^0 \mathbf{e}_n|^2}, \qquad n \in \chi \tag{22}$$

Using such regularization factor, the amplitude of peak-canceling signals $\mathbf{V}_n^0 \mathbf{e}_n$ generated by LSA, almost equal to those of the original clipping noise. Obviously, it may reduce the number of iterations to achieve a good PAPR reduction (see Section V).

However, the peak-canceling signals $\{\mathbf{V}_n^0 \mathbf{e}_n\}$ hardly equal to $\{\mathbf{d}_n\}$, because $|\chi| < N$. Then, we search, via the proposed algorithm, to optimize the solution $\dot{\mathbf{e}}_n$ according to the following simple convex optimization problem

$$\begin{aligned} &\underset{\dot{\mathbf{e}}_n}{minimize} \quad G(\mathbf{e}_n) = \|\mathbf{V}_n^0 \mathbf{e}_n - \mathbf{d}_n\|_2^2, \qquad n \in \chi \\ &subject \;\; to \qquad \dot{\mathbf{e}}_n = \mathbf{0}_{(M_t - M_r)\times 1}, \qquad n \in \chi^c \end{aligned} \tag{23}$$

Note that when $|\chi| = N$, (23) has a unique solution, i.e., $\dot{\mathbf{e}}_n = \mathbf{V}_n^{0\,\dagger} \mathbf{d}_n$, otherwise, it leads to a poor PAPR reduction meanwhile its computational complexity is very high since we have to compute the pseudo-inverse of an $M_t \times (M_t - M_r)$-dimensional matrix $\mathbf{V}_n^0$.

B. PROPOSED FORMULATION

Ideally, PAPR reduction is achieved by minimizing the l_∞-norm of the time-domain signals $\{\mathbf{a}_{m_t}^t, \forall m_t\}$. With taking into consideration constraints in (7) and (8), The MU precoding scheme based PAPR reduction is cast as

$$\begin{aligned} &\underset{\{\dot{\mathbf{a}}_{m_t}^t\}}{minimize} \quad \{\|\mathbf{a}_1^t\|_\infty, ..., \|\mathbf{a}_{M_t}^t\|_\infty\} \\ &subject \;\; to \begin{cases} \mathbf{s}_n = \mathbf{H}_n \mathbf{x}_n, & n \in \chi \\ \mathbf{x}_n = \mathbf{0}_{M_t \times 1}, & n \in \chi^c \end{cases} \end{aligned} \tag{24}$$

Since the solution of the l_∞-norm is in fact obtained by the clipping and control, as discussed in Section III-A, we are able to state the formulation in (24) subject to constraints (17) and (20) as a simple convex optimization problem

$$\begin{aligned} &\underset{\{\dot{\mathbf{e}}_n\}}{minimize} \quad G(\mathbf{e}_n) = \|\mathbf{V}_n^0 \mathbf{e}_n - \mathbf{d}_n\|_2^2, \qquad n \in \chi \\ &subject \;\; to \begin{cases} \mathbf{s}_n = \mathbf{H}_n \left(\mathbf{x}_n + \mathbf{V}_n^0 \mathbf{e}_n\right), & n \in \chi \\ \mathbf{x}_n = \mathbf{0}_{M_t \times 1}, & n \in \chi^c \\ \mathbf{e}_n = \mathbf{0}_{(M_t - M_r)\times 1}, & n \in \chi^c \end{cases} \end{aligned} \tag{25}$$

Note that the above formulation will yield an iterative CF algorithm with the peak-canceling signals constrained in the null-space of the associated MIMO channel matrices. The objective is to search for signals $\{\mathbf{e}_n\}$ which can help reduce the PAPR and meanwhile satisfy the MU precoding, in-band and out-of-band constraints. It is worth noticing that the proposed formulation can separate the PAPR reduction problem from the MU precoding by initializing precoded signals $\{\mathbf{x}_n\}$ according to a pre-fixed precoder or from a pre-specified codebook, and as a consequence, it is transparent to the precoding design.

IV. MU-PP-GDM ALGORITHM

In this section, we develop a new algorithm to find an effective solution to (25). The MU precoding scheme based PAPR reduction is achieved by alternately repeating the PAPR reduction process using the CF method, restoring the restrictions on the PAPR reduction signal components using null-space MIMO channels and performing MU precoding. To make the problem tractable, the equality constraint $\mathbf{s}_n = \mathbf{H}_n \left(\mathbf{x}_n + \mathbf{V}_n^0 \mathbf{e}_n\right)$, which is equivalent to $\mathbf{s}_n = \mathbf{H}_n \mathbf{x}_n$, is relaxed as

$$\begin{aligned} &\underset{\{\dot{\mathbf{e}}_n, \dot{\mathbf{x}}_n\}}{minimize} \quad J(\mathbf{x}_n, \mathbf{e}_n) = F(\mathbf{x}_n) + G(\mathbf{e}_n), \quad n \in \chi \\ &subject \;\; to \begin{cases} \mathbf{x}_n = \mathbf{0}_{M_t \times 1}, & n \in \chi^c \\ \dot{\mathbf{e}}_n = \mathbf{0}_{(M_t - M_r)\times 1}, & n \in \chi^c \end{cases} \end{aligned} \tag{26}$$

An alternating minimization strategy can be used to solve (26), in which we alternatively minimize the objective function with respect to $\mathbf{x}_n$ and $\mathbf{e}_n$. Thus in the $(l+1)$-th iteration, the alternating procedure can be expressed as

$$\mathbf{x}_n^{(l+1)} = \underset{\{\mathbf{x}_n\}}{argmin} \quad J(\mathbf{x}_n, \mathbf{e}_n^{(l)}), \qquad n \in \chi \tag{27}$$

$$\mathbf{e}_n^{(l+1)} = \underset{\{\mathbf{e}_n\}}{argmin} \quad J(\mathbf{x}_n^{(l+1)}, \mathbf{e}_n^{(l)}), \quad n \in \chi \tag{28}$$

By doing so, the constrained optimization problem is relaxed, which therefore enables low-complexity first-order algorithm, i.e., an algorithm only requires matrix-vector multiplications, such as the steepest gradient descent (GD) method [21] [22]. The proposed algorithm to solve (26) is referred to as MU-PP-GD.

The search directions of the steepest descent method at the iterate $\mathbf{x}_n^{(l)}$ and $\mathbf{e}_n^{(l)}$ are determined by the negative gradient of J at, respectively, $\mathbf{x}_n^{(l)}$ (denoted by $-\nabla_x^l J(\mathbf{x}_n^{(l)}, \mathbf{e}_n^{(l)})$) and $\mathbf{e}_n^{(l)}$ (denoted by $-\nabla_e^l J(\mathbf{x}_n^{(l+1)}, \mathbf{e}_n^{(l)})$), where

$$\nabla_x^l J(\mathbf{x}_n^{(l)}, \mathbf{e}_n^{(l)}) = \frac{2}{\mathcal{L}_{x_n}} \mathbf{H}_n^H \left(\mathbf{H}_n \mathbf{x}_n^{(l)} - \mathbf{s}_n\right), \quad n \in \chi \tag{29}$$

$$\nabla_e^l J(\mathbf{x}_n^{(l+1)}, \mathbf{e}_n^{(l)}) = \frac{2}{\mathcal{L}_{e_n}} \mathbf{V}_n^{0\,H} \left(\mathbf{V}_n^0 \mathbf{e}_n^{(l)} - \mathbf{d}_n^{(l+1)}\right), \quad n \in \chi \tag{30}$$

where $\mathcal{L}_{x_n} = 2\sigma^2_{max}(\mathbf{H}_n)$ and $\mathcal{L}_{e_n} = 2\sigma^2_{max}(\mathbf{V}^0_n)$ are the Lipschitz constants [23] for, respectively, $\|\mathbf{H}_n\mathbf{x}_n - \mathbf{s}_n\|_2^2$ and $\|\mathbf{V}^0_n\mathbf{e}_n - \mathbf{d}_n\|_2^2$.

In this work, we consider the gradient descent with momentum [24] in order to enhance the convergence rate of the algorithm. We do this by adding a fraction μ of the update vector of the past time step to the current update vector (the algorithm referred to as MU-PP-GDm).

A. ALGORITHM SUMMARY

The details of the proposed MU-PP-GDm is summarized in Tab. **Algorithm**. One can note that the proposed algorithm proceeds in only one-loop where it performs the precoded signals (Step 4) using gradients computed in Step 3, the peak-canceling signals in Step 6 and its constrained version in Step 7. Finally, in Step 9, the precoded signals are re-updated to take into consideration the peak-canceling signals, which are constrained to lie in the null-space of their associated MIMO channel matrices. Also, note that the constraints in (26) are always satisfied throughout the whole iterative process. Hence, any intermediate solution can be used, without causing any in-band or out-of-band radiations.

Algorithm: The MU-PP-GDm algorithm

Given a set of N modulated complex signals $\{\mathbf{s}_n\}$.

1: **Initialize** $\mathbf{x}_n^{(1)} = \mathbf{0}_{M_t\times 1}$,
$\mathbf{e}_n^{(1)} = \mathbf{0}_{(M_t-M_r)\times 1}$,
$\mathbf{dx}_n^{(0)} = \mathbf{0}_{M_t\times 1}$,
$Lx_n = 2\sigma^2_{max}(\mathbf{H}_n)$, $Le_n = 2\sigma^2_{max}(\mathbf{V}^0_n)$,
and set the maximal iteration number $maxIter$
and the momentum term μ

2: **for** l=1,...,$maxIter$ **do**

3: $\mathbf{dx}_n^{(l)} = \frac{2}{\mathcal{L}_{x_n}}\mathbf{H}_n^H\left(\mathbf{H}_n\mathbf{x}_n^{(l)} - \mathbf{s}_n\right) + \mu\mathbf{dx}_n^{(l-1)}, \quad \forall n \in \chi$

4: $\mathbf{x}_n^{(l+1)} = \mathbf{x}_n^{(l)} - \mathbf{dx}_n^{(l)}, \quad \forall n \in \chi$

5: $\mathbf{a}_{m_t}^{t(l+1)} = IFFT\left(\mathbf{x}_{m_t}^{t(l+1)}\right), \quad \forall m_t = 1...M_t$

6: $\mathbf{d}_{m_t}^{t(l+1)} = FFT\left(\tilde{\mathbf{a}}_{m_t}^{t(l+1)} - \mathbf{a}_{m_t}^{t(l+1)}\right)$

7: $\mathbf{e}_n^{t(l+1)} = \mathbf{e}_n^{t(l)} - \frac{2}{\mathcal{L}_{e_n}}\mathbf{V}_n^{0\,H}\left(\mathbf{V}^0_n\mathbf{e}_n^{(l)} - \mathbf{d}_n^{(l+1)}\right), \quad \forall n \in \chi$

8: $\mathbf{p}_n = \frac{\sum_k |\mathbf{V}^0_n\mathbf{e}_n^{(l+1)}||\mathbf{d}_n^{(l+1)}|}{\sum_k |\mathbf{V}^0_n\mathbf{e}_n^{(l+1)}|^2}, \quad \forall n \in \chi$

9: $\mathbf{x}_n^{(l+1)} = \mathbf{x}_n^{(l+1)} + \mathbf{p}_n\mathbf{V}^0_n\mathbf{e}_n^{(l+1)}, \quad \forall n \in \chi$

10: **end for**

11: **return** $\{\tilde{\mathbf{x}}_n = \mathbf{x}_n^{(maxIter+1)}\}$

B. COMPLEXITY ANALYSIS

We adopt the number of complex multiplications as a complexity measure to compare the complexity of the proposed algorithm with that of PROXINF-ADMM [12] and FITRA [10]. For the proposed MU-PP-GDm, we can easily verify that the computational cost is dominated by the gradients $\nabla^l_x J$ (Line 3), $\nabla^l_e J$ (Line 7) and the N-points IFFT/FFT (Lines 5 and 6). The gradient in line 3 of the algorithm involves $\mathcal{O}\left(2|\chi|M_tM_r\right)$ complex multiplications. Line 7 requires $\mathcal{O}\left(2|\chi|M_t(M_t - M_r)\right)$ complex multiplications for the second gradient. The IFFT/FFT costs $\mathcal{O}\left(M_tN\log\left(N\right)\right)$ complex multiplications. Therefore, the MU-PP-GDm requires a total of $\mathcal{O}\left(2M_tN\log\left(N\right) + 2|\chi|{M_t}^2\right)$ complex multiplications for each iteration. By contrast, the PROXINF-ADMM [12] needs $\mathcal{O}\left(|\chi|\left(M_r{M_t}^2\right)\right)$ for the initialization step and $\mathcal{O}\left(M_tN\log\left(N\right) + \mathbf{I}_{max}M_r|\chi|{M_t}^2\right)$ for each iteration [12], where $\mathbf{I}_{max}$ is the number iterations in the inner loop, that was flexed to 2 [12]. While, the FITRA requires about $\mathcal{O}\left(M_rM_tN^2\right)$ complex multiplications per iteration [12]. Evidently, the number of iterations needed to achieve a desirable PAPR performance will be of paramount importance in evaluating the complexity of these algorithms. Complexity comparison will be given, in the next section, where many PAPR performance levels are considered.

V. SIMULATION RESULTS

A. PERFORMANCE EVALUATION

To demonstrate the efficiency of the proposed algorithm for joint MU precoding and PAPR reduction, some simulations have been conducted in an OFDM-based MU massive MIMO system. This latter has $M_t = 100$ antennas at the BS and serving $M_r = 10$ single-antenna users. We consider an uncoded OFDM with $N = 128$ subcarriers and use a spectral map χ, in which $|\chi| = 114$ subcarriers are used for data transmission. A 16 quadrature amplitude modulation (16-QAM) with Gray mapping is considered. The number of FFT/IFFT points is set to 512, which corresponds to $L = 4$-oversampling in the time-domain in order to measure the PAPR levels accurately. We use the complementary cumulative distribution function (CCDF) to evaluate the PAPR reduction performance, which denotes the probability that the PAPR of the estimated signal exceeds a given threshold $PAPR_0$. Also, to evaluate the multi-user interference, we define the MUI as

$$MUI = \frac{\sum_{n\in\chi}\|\mathbf{H}_n\mathbf{x}_n - \mathbf{s}_n\|_2^2}{\sum_{n\in\chi}\|\mathbf{s}_n\|_2^2} \tag{31}$$

The wireless channel is assumed to be frequency-selective and modeled as a tap delay line with $T = 8$ taps. The time-domain channel response matrices $\mathbf{H}_t$, $t = 1, ..., T$, have i.i.d. circularly symmetric Gaussian distributed entries with zero mean and unit variance. The equivalent frequency-domain response $\mathbf{H}_n$ on the n-th subcarrier can be obtained by

$$\mathbf{H}_n = \sum_{t=1}^{T}\mathbf{H}_t e^{\frac{-j2\pi tn}{N}} \tag{32}$$

We compare our algorithm with the conventional ZF precoding scheme. It is worth to mention that all parameters used in our proposed algorithm are determined automatically

and no parameter is defined manually, expect if we add the momentum term which is set to be $\mu = 0.11$. In contrast to other existing algorithms, like FITRA [10] and PROXIINF-ADMM [12] where many parameters have to be fixed manually which is not straightforward in practical system. In our algorithm, λ (equation 19) and $\{\mathbf{p}_n\}$ (equation 22) are automatically adjusted in each iteration that offers the best convergence rate to the optimal PAPR [19] [20].

To evaluate the efficiency of our algorithm in term of PAPR reduction, Fig. 2 shows the CCDF of the PAPR when different numbers of iterations are considered. Note that PAPRs associated with all M_t antennas are taken into account in computing the empirical CCDF. The number of channel trials is chosen to be 1000 in our simulations. We note that our algorithm provides substantial PAPR reduction compared with the conventional ZF precoding scheme. Indeed, it achieves a gain of 5.7dB, 6dB and 6.3dB when, respectively, 10, 20 and 100 iterations are considered (at CCDF of 1%). We can also note that our algorithm, within few number of iterations (e.g. $maxIter = 20$) offers PAPR reduction performance similar than PROXIINF-ADMM and FITRA that need to perform, respectively, 40 and 1000 iterations. However, PROXIINF-ADMM and FITRA outperform our algorithm MU-PP-GD when a large number of iterations is performed, e.g. 200 and 2000 for, PROXIINF-ADMM and FITRA, respectively. However, this gain is at the cost of SNR loss, which causes the symbol error rate (SER) and capacity performance loss compared to the ZF scheme. This is undesirable in practical 5G and Beyond systems. This performance loss is primarily due to an increase in the norm of the obtained solution $\tilde{\mathbf{x}}$, i.e. increase in the transmit power $\|\tilde{\mathbf{x}}\|_2^2$. It is not surprising to see that the solution obtained by our proposed method has a smaller norm than the solution of PROXIINF-ADMM since our MU-PP-GDm algorithms aims at performing jointly the MU precoding (optimizing the same criterion as in ZF) and PAPR reduction. Therefore, MU-PP-GDm tends to converge to a norm solution very close to the ZF one.

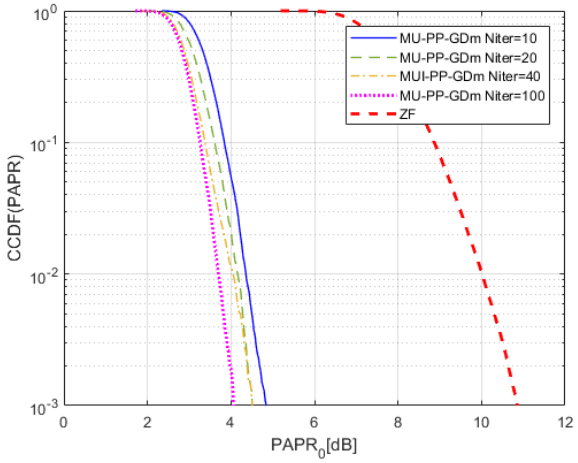

FIGURE 2. PAPR performance.

To confirm this point of view, we plot the SER performance of the proposed MU-PP-GDm algorithm in Fig. 3, where the SNR is defined as $SNR = \mathbb{E}\{\|\mathbf{x}_n\|_2^2\}/N_0$. In contrast to PROXIINF-ADMM and FITRA, we can note that our algorithm incurs a negligible SNR performance loss, e.g. at $SER = 10^{-3}$, 0.25dB of SNR loss is shown compared to the ZF scheme, even when the number of iteration is large ($maxIter = 200$).

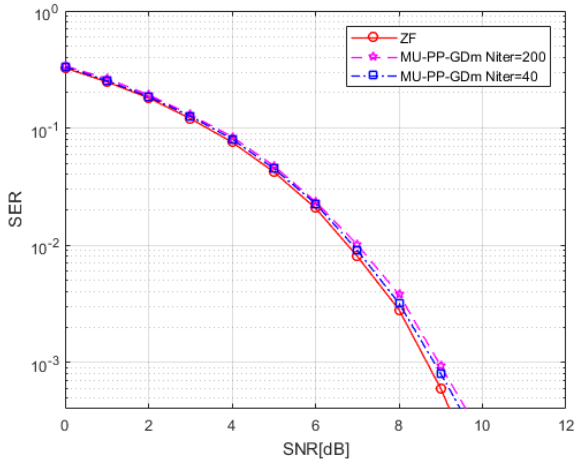

FIGURE 3. SER performance, 16-QAM.

We now discuss the convergence rate of the proposed MU-PP-GDm algorithm. Figs. 4 and 5 show, respectively, the MUI and the average PAPR versus the number of iterations. We note that our algorithm achieves a MUI of about -308dB with only 30 and 80 iterations which corresponds, respectively, to the use of the gradient descent with or without momentum. We can also note that MU-PP-GDm can achieve a MUI of about -100dB when only 10 iterations are performed, which is a sufficient performance needed in practical systems. Moreover, our method has a low computational complexity since this MUI is performed using simple first-degree algorithm (using matrix-vector multiplications) which needs $\mathcal{O}(2M_tM_r)$ per iteration. With this few number of iterations needed, its computational complexity is considerably lower than initializing the precoded signal using ZF scheme (the solution adopted by PROXINF-ADMM) which has to compute the pseudo-inverse of a large-scale matrix. We move now to the PAPR, one can note that our proposed MU-PP-GDm performs well when the optimal solutions of $\{\mathbf{p}_n\}$ is considered. We can clearly see a gain of about 100 iterations for an achieved PAPR of 3dB (see Fig. 6). The proposed MU-PP-GDm can obtain a PAPR of 4dB with only 6 iterations, while PROXINF-ADMM and FITRA algorithms require 20×2 (outer loop and inner loop) and 800 iterations, respectively. Also, the proposed algorithm is able to reduce the PAPR down to 3dB with only 40 iterations, while the PROXINF-ADMM and FITRA require 100 and 1500 iterations, respectively, to obtain a similar result. It is worth to mention that the PROXINF-ADMM and FITRA algorithms

converge to a lower PAPR than the proposed MU-PP-GDm but at the cost of transmission quality loss. This means that the MU-PP-GDm has the fastest convergence rate compared to PROXINF-ADMM and FITRA but a higher PAPR that does not affect a lot the transmission quality. This trade-off between PAPR reduction and transmission quality loss is assured by the joint performing of MU precoding and PAPR reduction. It is worth mentioning that the proposed algorithm is as sensitive to the inaccuracy of the channel state information (CSI) as the ZF scheme.

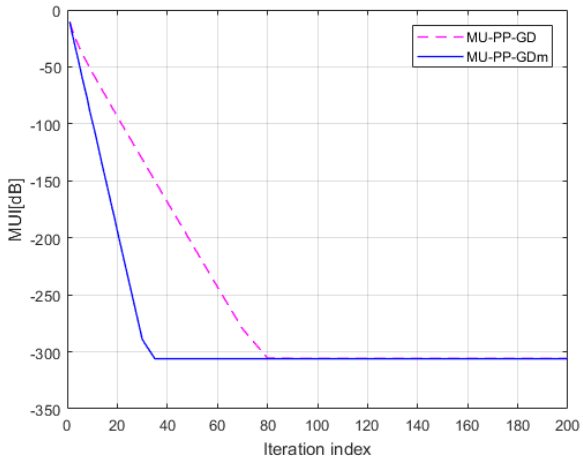

FIGURE 4. Convergence rate of MUI.

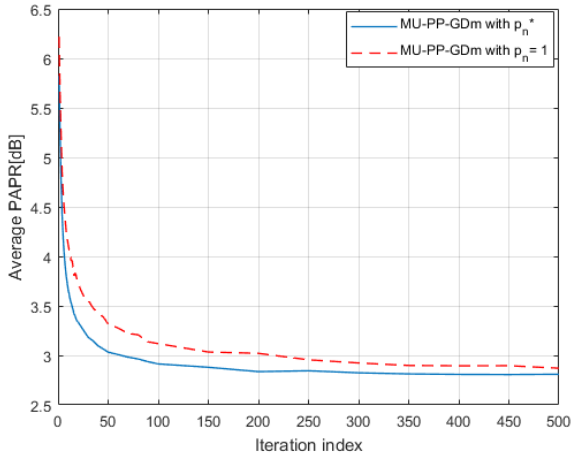

FIGURE 5. Convergence rate of PAPR.

Finally, we examine the efficiency of our proposed algorithm under different number of transmit antennas (varies from 20 to 120), while the number of users is fixed to be $M_r = 10$. Here, we would like to show the effect of DoF offered by equipping the BS by a large number of antennas on the performance of our algorithm. Figs. 6 and 7 illustrates, respectively, the MUI and the PAPR versus the number of transmit antennas, where different numbers of iterations are considered. Results are averaged over 1000 independent simulations and PAPR results are averaged over PAPRs associated with all transmit antennas. We observe that the number of iterations required to achieve a given MUI increases as the number of antennas decreases, e.g. for a MUI of -200dB, about 20, 40 and 80 iterations are required for $M_t = 100$, $M_t = 80$ and $M_t = 40$. We can explain this by the fact that the proposed algorithm achieves better MUI performance when more DoF at the base station are available.

We move now to the PAPR (Fig. 7), one can note that the MU-PP-GDm can achieve lower PAPR when the null-space of the MIMO channel is larger (with higher number of transmit antennas), i.e. more DoF at the base station are available.

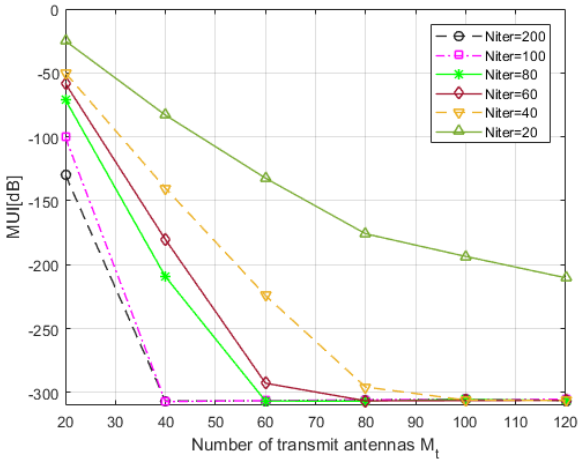

FIGURE 6. MUI vs. number of transmit antennas.

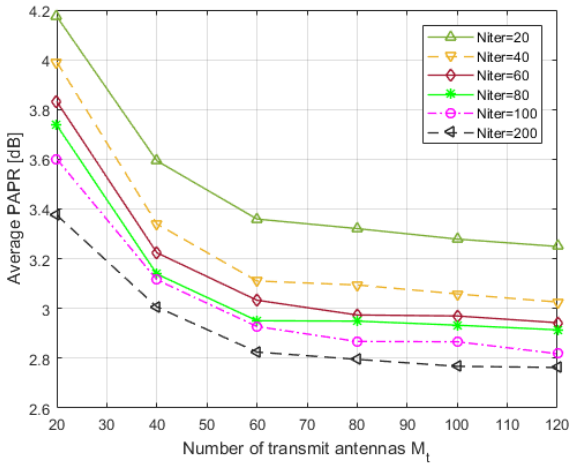

FIGURE 7. PAPR vs. number of transmit antennas.

Simulation results showed that MU-PP-GDm is able to achieve substantial PAPR reduction performance, without affecting at all the MUI and the out-of-band radiations, meanwhile providing a faster convergence rate compared to the existing algorithms. This could substantially motivate the use of low-cost and low-size radio-frequency (RF) components

TABLE 1. Complexity Comparison

Algo.	**Complexity per iteration**	**Complexity to achieve a PAPR of 4dB**	**Complexity to achieve a PAPR of 3dB**
FITRA [10]	16384000	1.3107×10^{10}	2.4576×10^{10}
PROXINF-ADMM [12]	34379200	470984000	2.3093×10^{9}
Proposed MU-PP-GDm	2459200	14755200	98368000
$\frac{\mathcal{O}(\mathbf{MU-PP-GDm})}{\mathcal{O}(\mathbf{PROXINF-ADMM})}$	7.15%	3.13%	4.26%
$\frac{\mathcal{O}(\mathbf{MU-PP-GDm})}{\mathcal{O}(\mathbf{FITRA})}$	15.01%	0.1%	0.4%

in future wireless massive MIMO-OFDM communication systems.

B. COMPLEXITY COMPARISON

According to the aforementioned closed-form expressions (see Section IV-B) and the configuration given in Section V-A, it is possible to numerically assess the complexity of the proposed MU-PP-GD algorithm. The comparison with the existing algorithms, PROXINF-ADMM [12] and FITRA [10], is given in Tab. 1. We consider to compute the complexity required by each algorithm (1) for one iteration, (2) to achieve an average PAPR of 4dB and (3) to achieve an average PAPR of 3dB. As discussed in Section V-A, to achieve an average PAPR of 4dB, the MU-PP-GDm, PROXINF-ADMM and FITRA require 6, 20 and 800 iterations, respectively. While to achieve an average PAPR of 4dB, they need 40, 100 and 1500 iterations, respectively. We have considered these iteration numbers to numerically assess the complexity of each algorithm.

According to results illustrated in Tab. 1, we can easily note that MU-PP-GDm algorithm complexity is substantially less than that of the two considered algorithms. Note that the energy-efficiency refers to the trade-off between the PAPR reduction gain and the computational complexity of the associated method [25]. Thus, our proposed algorithm provides better energy-efficiency among the other algorithms.

The comparison of the proposed MU-PP-GDm algorithm to FITRA [10] and PROXINF-ADMM [12] ones is summarized in Tab. 2, where we illustrate the enormous advantages of our proposed scheme compared to these methods.

VI. CONCLUSION

In this paper, we investigated the joint MU precoding and PAPR reduction in OFDM based massive MIMO downlink systems. We developed an algorithm to perform jointly the MUI interference cancellation and PAPR reduction. The proposed algorithm, referred to as MU-PP-GDm, facilitates an explicit trade-off between PAPR and transmission quality. The motivation of MU-PP-GDm is the high-dimensional null-space associated to the massive MIMO downlink channel matrix, which enables as to device transmit signals with low PAPR while maintaining excellent transmission quality. The joint MU precoding and PAPR reduction scheme was formulated as a simple convex optimization problem for which an algorithm based steepest gradient descent method was designed. The MU-PP-GDm only involves simple matrix-vector multiplications at each iteration, leading then to the lowest computational complexity among all existing algorithms. A possibility for future work is to extend this algorithm to take into consideration, in addition to the PAPR reduction, other RF impairments (like PA non-linearity,...).

REFERENCES

[1] T. L. Marzetta. Noncooperative cellular wireless with unlimited numbers of base station antennas. IEEE Transactions on Wireless Communications, 9(11):3590–3600, November 2010.
[2] E. G. Larsson, O. Edfors, F. Tufvesson, and T. L. Marzetta. Massive mimo for next generation wireless systems. IEEE Communications Magazine, 52(2):186–195, February 2014.
[3] H. Q. Ngo, E. G. Larsson, and T. L. Marzetta. Energy and spectral efficiency of very large multiuser mimo systems. IEEE Transactions on Communications, 61(4):1436–1449, April 2013.
[4] C. Mollén, E. G. Larsson, and T. Eriksson. Waveforms for the massive mimo downlink: Amplifier efficiency, distortion, and performance. IEEE Transactions on Communications, 64(12):5050–5063, Dec 2016.
[5] K. N. R. S. V. Prasad, E. Hossain, and V. K. Bhargava. Energy efficiency in massive mimo-based 5g networks: Opportunities and challenges. IEEE Wireless Communications, 24(3):86–94, June 2017.
[6] S. K. Mohammed, A. Chockalingam, and B. S. Rajan. A low-complexity precoder for large multiuser miso systems. In VTC Spring 2008 - IEEE Vehicular Technology Conference, pages 797–801, May 2008.
[7] Christian Siegl and Robert FH Fischer. Selected basis for par reduction in multi-user downlink scenarios using lattice-reduction-aided precoding. EURASIP Journal on Advances in Signal Processing, 2011(1):17, Jul 2011.
[8] H. Prabhu, O. Edfors, J. Rodrigues, L. Liu, and F. Rusek. A low-complex peak-to-average power reduction scheme for ofdm based massive mimo systems. In 2014 6th International Symposium on Communications, Control and Signal Processing (ISCCSP), pages 114–117, May 2014.
[9] C. Ni, Y. Ma, and T. Jiang. A novel adaptive tone reservation scheme for papr reduction in large-scale multi-user mimo-ofdm systems. IEEE Wireless Communications Letters, 5(5):480–483, Oct 2016.
[10] C. Studer and E. G. Larsson. Par-aware large-scale multi-user mimo-ofdm downlink. IEEE Journal on Selected Areas in Communications, 31(2):303–313, February 2013.
[11] H. Bao, J. Fang, Z. Chen, H. Li, and S. Li. An efficient bayesian papr reduction method for ofdm-based massive mimo systems. IEEE Transactions on Wireless Communications, 15(6):4183–4195, June 2016.
[12] H. Bao, J. Fang, Q. Wan, Z. Chen, and T. Jiang. An admm approach for papr reduction for large-scale mimo-ofdm systems. IEEE Transactions on Vehicular Technology, 67(8):7407–7418, Aug 2018.
[13] S. Sun, B. Rong, R. Q. Hu, and Y. Qian. Spatial domain management and massive mimo coordination in 5g sdn. IEEE Access, 3:2238–2251, 2015.
[14] Q. Qin, L. Gui, B. Gong, and S. Luo. Sparse channel estimation for massive mimo-ofdm systems over time-varying channels. IEEE Access, 6:33740–33751, 2018.
[15] L. Lu, G. Y. Li, A. L. Swindlehurst, A. Ashikhmin, and R. Zhang. An overview of massive mimo: Benefits and challenges. IEEE Journal of Selected Topics in Signal Processing, 8(5):742–758, Oct 2014.
[16] G. Chen, Q. Zeng, X. Xue, and Z. Li. A low complexity precoding algorithm based on parallel conjugate gradient for massive mimo systems. IEEE Access, 6:54010–54017, 2018.

TABLE 2. Downlink Transmission Schemes : Comparison Summary

Algo.	**Advantages**	**Disadvantages**
FITRA [10]	Low PAPR	Slow convergence rate High complexity Non null MUI Non null OBR Appropriate regularization parameters are needed CSI is needed
PROXINF-ADMM [12]	Low PAPR Null MUI Null OBR	Quite fast convergence rate High complexity Appropriate regularization parameters are needed Requires inversion of $M_r \times M_r$ matrices CSI is needed
Proposed MU-PP-GDm	Low PAPR Null MUI Null OBR Fast convergence rate All parameters are adjusted automatically	CSI is needed

[17] C. Zhang, Z. Li, L. Shen, F. Yan, M. Wu, and X. Wang. A low-complexity massive mimo precoding algorithm based on chebyshev iteration. IEEE Access, 5:22545–22551, 2017.

[18] H. Sun, J. Guo, and L. Fang. Improved singular value decomposition (topsvd) for source number estimation of low snr in blind source separation. IEEE Access, 5:26460–26465, 2017.

[19] T. Jiang, C. Ni, C. Xu, and Q. Qi. Curve fitting based tone reservation method with low complexity for papr reduction in ofdm systems. IEEE Communications Letters, 18(5):805–808, May 2014.

[20] H. Li, T. Jiang, and Y. Zhou. An improved tone reservation scheme with fast convergence for papr reduction in ofdm systems. IEEE Transactions on Broadcasting, 57(4):902–906, Dec 2011.

[21] X. Qin, Z. Yan, and G. He. A near-optimal detection scheme based on joint steepest descent and jacobi method for uplink massive mimo systems. IEEE Communications Letters, 20(2):276–279, Feb 2016.

[22] Weishui Wan. Implementing online natural gradient learning: problems and solutions. IEEE Transactions on Neural Networks, 17(2):317–329, March 2006.

[23] G.H. Golub and C. F. van Loan. Matric Computations, 3rd edition, johns hopkins univ., sweden,.

[24] A. Botev, G. Lever, and D. Barber. Nesterov's accelerated gradient and momentum as approximations to regularised update descent. In 2017 International Joint Conference on Neural Networks (IJCNN), pages 1899–1903, May 2017.

[25] Y. Louet, D. Roviras, A. Nafkha, H. Shaiek, and R. Zayani. Global power amplifier efficiency evaluation with papr reduction method for post-ofdm waveforms. In 2018 15th International Symposium on Wireless Communication Systems (ISWCS), pages 1–5, Aug 2018.

RAFIK ZAYANI (M'09) received the Engineer, M.Sc. and Ph.D. degrees from the Ecole Nationale dâĂŹIngenieurs de Tunis (ENIT) in 2003, 2004, and 2009, respectively. He was with the Laboratory of Communications Systems (SysâĂŹCom), ENIT, from 2003 to 2005. Since 2005, he has been with the InnovâĂŹCOM laboratory, SupâĂŹCom School, Tunisia. From 2004 to 2009, he was with the Department of Telecommunication and Networking, Institut SupÃľrieur dâĂŹInformatique (ISI), Tunis, as a contractual Assistant Professor. Since 2009, he has been an Associate Professor (tenure position) with the ISI, Tunisia. Since 2010, he has been an Associate Researcher with the CEDRIC Laboratory, Conservatoire National des Arts et Metiers, France. He is an Established Researcher with long experience in multicarrier communications, energy efficiency enhancement by: transmitter linearization techniques (baseband DPD) and PAPR reduction; high power amplifier characterization; neural network; identification modeling and equalization; and MIMO technologies. He was involved in enhanced multicarrier waveforms, such as FBMC-OQAM, UFMC, GFDM, BF-OFDM, and WOLA-OFDM. He has contributed in several European (EMPHATIC) and French (WONG5) projects that aim at designing flexible air-interfaces for future wireless communications (5G and Beyond). He has recently been awarded a H2020 Marie Sklodowska-Curie Actions (MSCA) Individual Fellowships (IF) grant for his ADMA5 project proposal.

HMAIED SHAIEK received the Engineer degree from the National Engineering School of Tunis in 2002, and the masterâĂŹs degree from the University of Bretagne Occidentale in 2003, and the Ph.D. degree from the Lab-STICC CNRS Team, Telecom Bretagne, in 2007. He was with Canon Inc., until 2009. He left the industry to integrate with the ÃL'cole Nationale dâĂŹIngenieurs de Brest as a Lecturer, from 2009 to 2010. In 2011, he joined the CNAM, as an Associate Professor in electronics and signal processing. He has authored or co-authored three patents, six journal papers, and over 25 conference papers. His research activities focus on performances analysis of multicarrier modulations with nonlinear power amplifiers, PAPR reduction, and power amplifier linearization. He contributed to the FP7 EMPHATIC European project and is involved in two national projects, such as Accent5 and Wong5, funded by the French National Research Agency. He has co-supervised three Ph.D. students and four master students.

DANIEL ROVIRAS was born in 1958. He received the Engineer degree from SUPELEC, Paris, France, in 1981, and the Ph.D. degree from the National Polytechnic Institute of Toulouse, Toulouse, France, in 1989. He spent in the industry as a Research Engineer for seven years. He joined the Electronics Laboratory, Ecole Nationale Superieure dâĂŹElectrotechnique, dâĂŹElectronique, dâĂŹInformatique, et des Telecommunications (ENSEEIHT). In 1992, he joined the Engineering School, ENSEEIHT, as an Assistant Professor, where he has been a Full Professor since 1999. Since 2008, he has been a Professor with the Conservatoire National des Arts et MÃl'tiers (CNAM), Paris, France, where his teaching activities are related to radio-communication systems. He is currently a member of the CEDRIC Laboratory, CNAM. His research activity was first centered around transmission systems based on infrared links. Since 1992, his topics have widened to more general communication systems, such as mobile and satellite communications systems, equalization, and predistortion of nonlinear amplifiers, and multicarrier systems.